Monatshefte für Chemie 123, 757–768 (1992)

Monatshefte für Chemie
Chemical Monthly

Complete ^{1}H- and ^{13}C-NMR Spectroscopic Assignment of Two Pentadecapeptides by Reverse C,H Correlation Techniques

Hermann Kalchhauser[1,*], **Martin Kriech**[1], **Horst Ahorn**[2], and **W. Sommergruber**[2]

[1] Department of Organic Chemistry, University of Vienna, A-1090 Wien, Austria
[2] Ernst-Boehringer-Institut für Arzneimittelforschung, A-1120 Wien, Austria

Summary. Two oligopeptides representing a wild type and a modified version of the polyprotein cleavage region for proteinase *2A* of the human rhinovirus type 2 (HRV2 *2A*) have been investigated using homo- and heterocorrelated 2D NMR spectroscopy. Proton-detected C,H correlation techniques turned out to be extremely useful for sequential resonance assignment. In one case, the complete amino acid backbone could be analyzed without using NOESY spectra, thus avoiding ambiguities inherent to this method. No defined tertiary structure of the cleavage region could be detected in either molecule. However, one of the oligopeptides is present to a very low extent in a conformation different from the *random-coil* arrangement.

Keywords. Virus; Peptide; NMR; Assignment; Reverse Techniques; Conformation.

Vollständige ^{1}H- und ^{13}C-NMR-spektroskopische Zuordnung von zwei Pentadecapeptiden mittels invers detektierter C,H-Korrelationstechniken

Zusammenfassung. Zwei Oligopeptide, die die native Spaltregion für die Proteinase *2A* des humanen Rhinovirus von Serotyp 2 (HRV2 *2A*) beziehungsweise eine modifizierte Version repräsentieren, wurden mit Hilfe von homo- und heterokorrelierter 2D-NMR-Spektroskopie untersucht. Protondetektierte C,H-Korrelationstechniken erwiesen sich als außerordentlich hilfreich bei der sequenziellen Zuordnung. In einem Fall konnte das gesamte Aminosäureskelett ohne Zuhilfenahme von NOESY-Spektren analysiert und damit die dieser Methode inhärenten Unsicherheiten bei der Zuordnung vermieden werden. In keinem der beiden Moleküle konnte eine definierte Tertiärstruktur der Spaltregion ermittelt werden. Eines der beiden Oligopeptide liegt jedoch zu einem sehr geringen Prozentsatz in einer von der *random-coil* Anordnung abweichenden Konformation vor.

Introduction

A variety of eukaryotic viruses produce their own virus specific proteinases which are involved in the maturation of viral protein precursors and/or in proteolytic modifications of host cell proteins [1]. Rhino- and enteroviruses belonging to the family of picornaviruses are completely dependent on specific proteolytic cleavages

of their polyproteins during their life cycle [2]. The polyprotein is synthesized from a single open reading frame coding for about 2100 amino acids [3–5]. In rhinoviruses (the main causative agents of common cold) and polioviruses, the first proteolysis is carried out by the viral protein *2A* which cleaves intramolecularly at its own N-terminus [6, 7]. Since the polyprotein is normally not observed in infected cells, it is very likely that this cleavage occurs on the growing peptide chain [8]. All but one of the remaining cleavages within the polyprotein (at least in rhino- and enteroviruses) are catalyzed by the second virus-encoded proteinase *3C* or its precursor *3CD*, respectively [6, 9].

Mechanistically, the *2A* and *3C* proteinases have a cystein residue as the active site nucleophile; however, the sequence surrounding it has a high similarity to that of serine proteinases [7, 10]. Recently, it has been proposed that *2A* and *3C* proteinases are structurally related to trypsin-like serine proteinases although there is only limited sequence homology [11, 12]. At present, there are no three-dimensional molecular structures of these viral proteins available.

The proteolytic enzymes involved in the processing of the polyprotein are highly substrate specific and seem to recognize a cleavage region (structural domain) rather than a certain cleavage signal represented by a single amino acid pair [2–4, 13]. Due to their substrate specificity and the catalytic mechanism, these proteinases offer a possibility of interfering therapeutically with the viral growth [14]. Regarding the fact that no vaccine against rhinoviruses can be designed for technical reasons (more than one hundred cross-reacting serotypes are known by now), the development of a proteinase inhibitor as an antiviral agent is of uttermost importance.

As knowledge of molecular conformation is essential to the understanding of biological activity [15], a first step towards this goal consists of correlating structure and function of the cleavage region of the polypeptide chain. We have therefore synthesized two different peptides and submitted the compounds to NMR spectroscopic analysis. Both of them can be cleaved quite efficiently by HRV2 *2A*. **1** resembles the native cleavage junction of HRV2 *2A* (cleaved at the Ala^7-Gly^8 amino acid pair). **2** also represents the HRV2 *2A* cleavage region except that the poliospecific cleavage signal Tyr^{10}-Gly^{11} has been introduced. The final aim of this investigation was the identification of a defined tertiary structure of the cleavage region of the rhino- and poliovirus, respectively.

1: H_2N-Arg^1-Pro^2-Ile^3-Ile^4-Thr^5-Thr^6-Ala^7-Gly^8-Pro^9-Ser^{10}-Asp^{11}-Met^{12}-Tyr^{13}-Val^{14}-His^{15}-NH_2

2: H_2N-Ile^1-Val^2-Thr^3-Arg^4-Pro^5-Ile^6-Ile^7-Thr^8-Thr^9-Tyr^{10}-Gly^{11}-Pro^{12}-Ser^{13}-Asp^{14}-Met^{15}-NH_2

Methods

The present method of choice for the evaluation of peptide conformations in aqueous solution, NMR spectroscopy at high magnetic fields, makes use of features well known from other fields of NMR spectroscopy, e. g. the Karplus relationship, the temperature dependence of the chemical shift of amide protons and, above all, the nuclear Overhauser effect [16]. Their application, however, relies firmly on a correct and unambiguous proton assignment. The usual method of assigning the

proton resonances with the help of *through-space* connectivities, especially H-C(α)$_i$ → NH$_{i+1}$, suffers from the severe drawback that no *a priori* decision can be made if an observed nuclear Overhauser effect originates from the neighbouring amino acid or from a residue located far away in terms of the linear backbone but nearby in a spatial sense because of the formation of a defined tertiary structure. The error arising from this ambiguity amounts to about 10−20% and can be minimized using suitable assignment strategies [17]. On the other hand, the exclusive application of unequivocal proton-proton *through-bond* connectivities for assignment purposes is made impossible by the carbonyl group separating the coupling network of neighbouring amino acid residues from each other, and the use of the backbone carbon atoms to overcome this problem is prevented by the low sensitivity and rare natural abundance of the ^{13}C isotope. Nevertheless, proton-carbon correlation techniques are extremly helpful for the disentangling of overlapping resonances in the proton domain and have therefore been used for assignment purposes of cyclic peptides in relatively concentrated nonaqueous solutions [18].

The advent of proton-detected heteronuclear 2D NMR techniques [19] dramatically improved the sensitivity of heteronuclei. Consequently, the new methods were almost immediately applied to the structure elucidation of peptides [20]. In the present paper, we want to demonstrate the utility of the new strategies for the NMR spectroscopic assignment of medium-sized oligopeptides in aqueous solution under physiological conditions.

Results and Discussion

Figure 1 illustrates the connectivity pathways employed by the more common 2D NMR techniques for structure elucidation in organic chemistry. Only one of these, i.e. the C,H-COSY experiment optimized for long-range couplings, fulfills the need of connecting neighbouring amino acid residues *via* the carbonyl group, yielding the assignment of the carbonyl carbon atom as a by-product. As a rule, not all connectivities can be extracted from the same experiment due to the nonequal $^2J_{CH}$ coupling constants between the various quarternary carbon atoms and the corresponding H-C(α) and NH protons. This is especially true for the H-C(α)/CO region where in addition to the loss of intensity caused by non-optimal measurement conditions the signal to noise ratio is usually poor because of the broad splitting patterns of the α-protons in the ^1H domain. In some cases, cross peaks between an H-C(β) and the corresponding carbonyl carbon atom ($^3J_{CH}$) can substitute

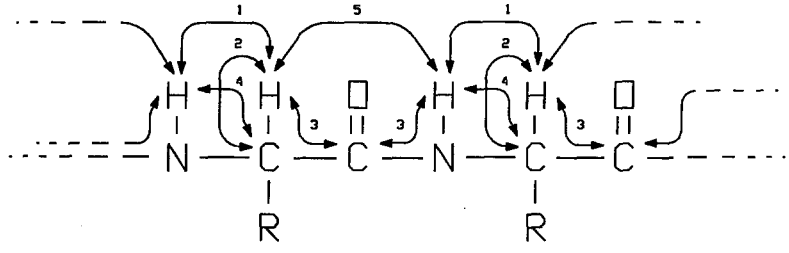

Fig. 1. Application of common 2D NMR techniques to the sequential assignment of amino acid residues in peptides. *1*: H,H-COSY (*via* $^3J_{H,H}$); *2*: C,H-COSY (*via* $^1J_{C,H}$); *3*: long-range C,H-COSY (*via* $^2J_{C,H}$); *4*: relayed C,H-COSY (*via* $^3J_{H,H}$ and $^1J_{C,H}$); *5*: NOESY (through-space)

missing H-C(α)-CO links (cf. Fig. 5). Another possibility of circumventing this problem is the recording of a series of spectra optimized for different coupling constants. The enormous value of the method in connecting the carbonyl carbon atom of residue (*i*) with the amide proton of residue (i+1) is shown in Fig. 2.

A consequent application of long-range C,H correlated spectra on the assignment of peptides involves a H,H-COSY step from the amide proton to H-C(α) in

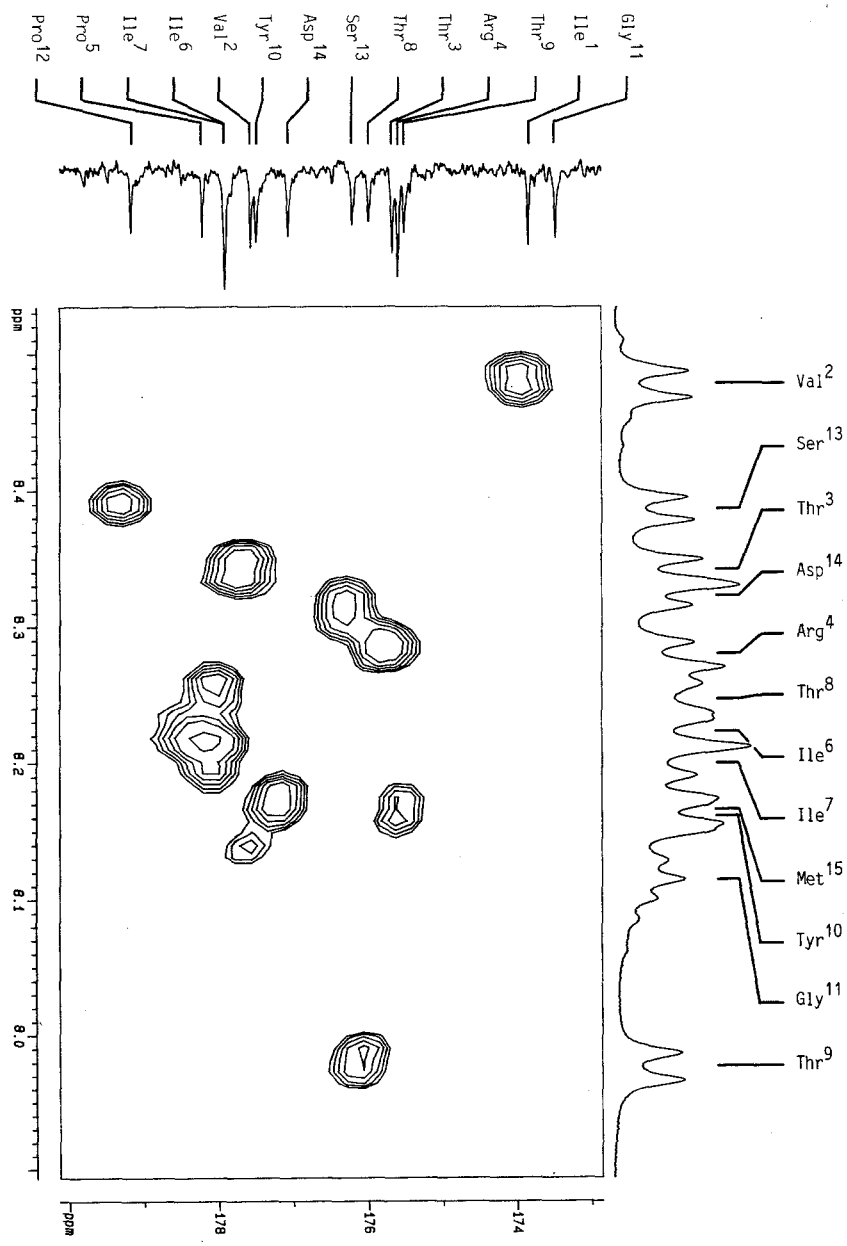

Fig. 2. Proton-detected long-range C,H-COSY spectrum optimized for $^2J_{C,H} = 10$ Hz of compound **2**. ω_1: carbonyl region; ω_2: amide region. Carbonyl carbon resonances of amino acid residues located prior to a proline in the peptide chain can be identified by the missing cross peak (Arg^4, Gly^{11}). The carbonyl carbon resonance of Met^{15} is situated outside of the shown region (180.66 ppm)

each residue. Severe overlap of signals both in the amide and α regions can make this task difficult to perform. An elegant method of avoiding this problem consists in recording a relayed C,H-COSY spectrum which uses a connectivity of NH and C(α) of the same amino acid *via* H-C(α) and therefore transfers the assignment problem to the heteronuclear domain, taking advantage of the large chemical shift dispersion of the ^{13}C nucleus compared to ^{1}H (Fig. 3).

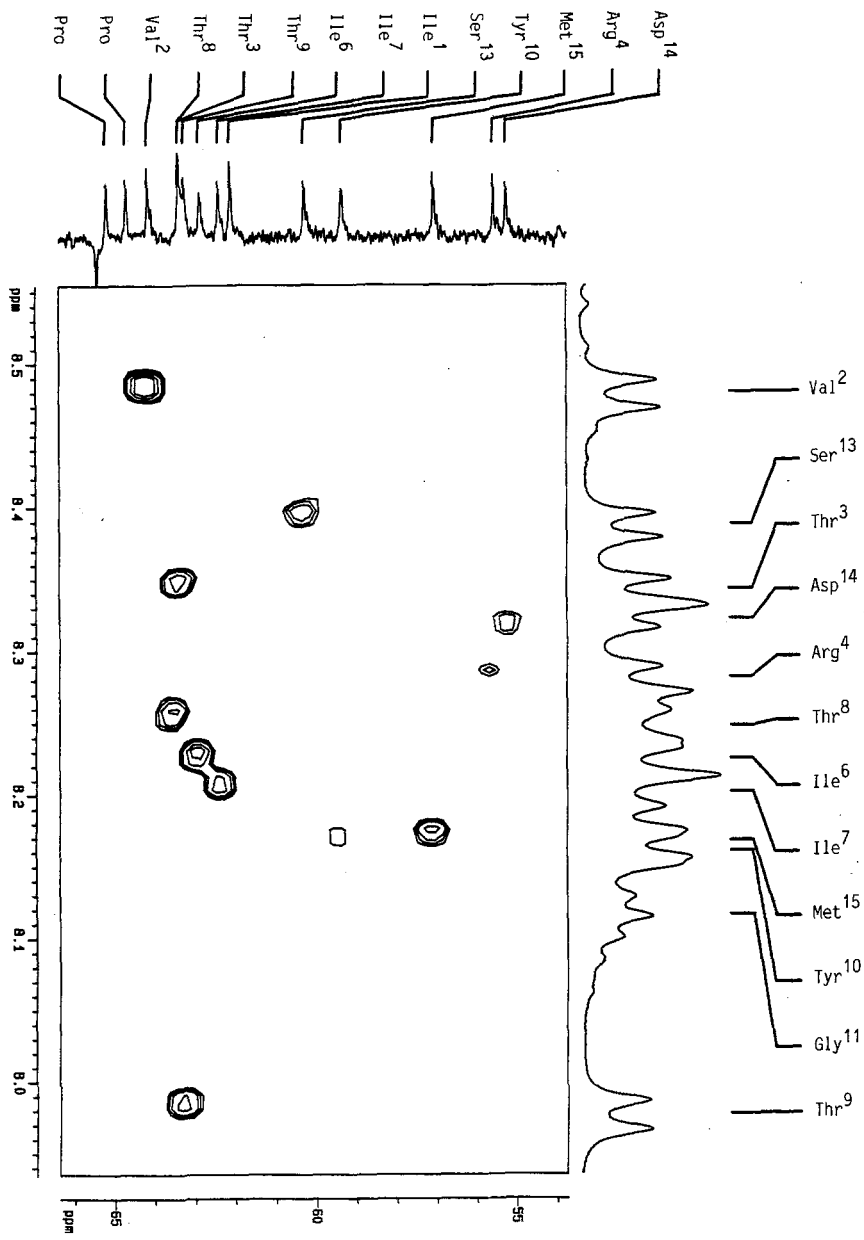

Fig. 3. Proton-detected relayed C,H-COSY spectrum of compound **2**. ω_1: C(α) region; ω_2: amide region. C(α) resonances of prolines can be identified by the missing cross peak. The C(α) resonance of Gly[11] is situated outside of the shown region (46.34 ppm). Note the improvement of peak shapes as compared to Fig. 2 due to the phase sensitive representation

In addition to their great value for the sequential assignment of amino acids, long-range and relayed C,H-COSY spectra afford information concerning prolines. Whereas C(α) signals of prolines can be traced out by the absence of a cross peak in the relayed C,H-COSY spectrum due to their tertiary nitrogen atom (cf. Fig. 3), the same principle applies to the carbonyl carbons of amino acid residues sequentially located prior to a proline residue in the long-range C,H-COSY experiment (e. g. Arg^4 and Gly^{11} in **2**; cf. Fig. 2).

The ideal way of stepping along the backbone of a peptide by NMR spectroscopy using exclusively heteronuclear through-bond connectivities therefore consists of four consecutive steps as depicted in Fig. 4. In practice, usually additional long-range C,H-COSY interactions (*vide supra*) have to be taken into consideration. In most cases, redundant connectivities can be found and serve as a control mechanism for the correctness of the assignments. The H,H-COSY experiment, however, is more or less obsolete for backbone analysis in this context and has been used mainly for corroborating the results deduced from C,H-COSY experiments and, of course, for the assignment of side chain protons. As an example, Figure 5 shows the assignment procedure for part of **2**, starting from Ser^{13}-C(β) which can easily be identified by its multiplicity and its characteristic shift value in the *J*-modulated ^{13}C-NMR spectrum. Further suitable entry points in the ^{13}C domain are, among others, Tyr-C(4′), Thr-C(β), Arg-C(ε), and His-C(1). It should be noticed at this point, however, that oligopeptides of the size of **1** and **2** at concentrations as given in the experimental part approach the limit at which it becomes hard to get a 1 D ^{13}C-NMR spectrum in reasonable time. With **1** and **2**, measurement times for the ^{13}C-NMR spectra were considerably longer than those necessary for the C,H-COSY experiment (cf. experimental part), and signal to noise ratios were only about 15 for aliphatic carbons and about 5 for α- and carbonyl carbon atoms.

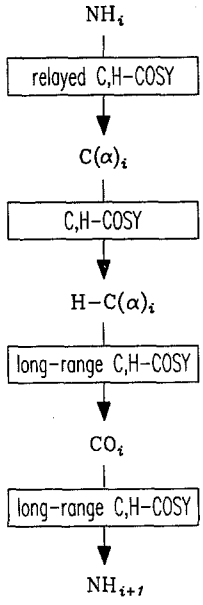

Fig. 4. Idealized scheme of the sequential NMR spectroscopic assignment procedure of a peptide backbone using exclusively heteronuclear correlation techniques

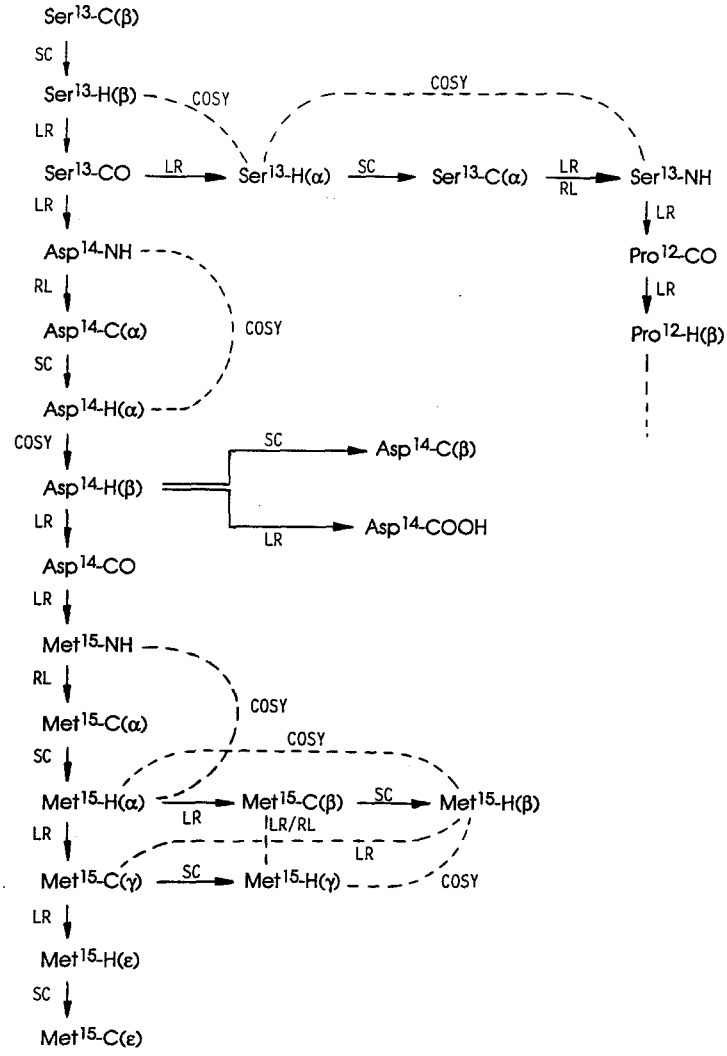

Fig. 5. Assignment procedure for part of compound **2**. *Entry point*: Ser^{13}-C(β); *COSY* H,H-COSY; *SC* C,H-COSY; *LR* long-range C,H-COSY; *RL* relayed C,H-COSY; *arrows*: connectivities used for resonance assignment; *dotted lines*: redundant connectivities. Note that the H,H-COSY experiment has been used only once in the sequence shown [Asp^{14}-H(α) → Asp^{14}-H(β)]

Proceeding according to the scheme described above, all ^1H and ^{13}C resonances of peptides **1** and **2** could be assigned (Tables 1 – 4). Cross peaks from NOESY experiments could therefore be used without any restriction for the establishment of a potential tertiary structure. However, both compounds did not exhibit through-space interactions beyond the trivial ones ($i \rightarrow i+1$) which were in accordance with the assignments found from heteronuclear correlation techniques. The proton chemical shifts which resemble closely the random coil values given in Ref. [17], and the equivalence of the ^{13}C chemical shifts of Tyr-C(2′,6′) and Tyr-C(3′,5′), respectively, in both **1** and **2** also can be used as arguments against a defined tertiary structure of the cleavage regions. However, additional small resonances which appear in both the ^1H- and ^{13}C-NMR spectra of **2** indicate that this compound is

Table 1. ^{1}H chemical shifts of **1** in H_2O:D_2O = 4 : 1 (3 m*M*) at 300 K relative to external *TMS*

	NH	α	β	γ	δ
Arg[1]		4.39	1.94	1.71	3.25[a]
			1.98	1.75	
Pro[2]		4.53	1.87	2.03	3.61
			2.34		3.76
Ile[3]	8.39	4.14	1.87	1.20	0.85[b]
				1.51	
Ile[4]	8.28	4.31	1.85	1.20	0.87[b]
				1.51	
Thr[5]	8.37	4.47	~4.2	1.20	
Thr[6]	8.15	4.37	~4.2	1.20	
Ala[7]	8.35	4.40	1.41		
Gly[8]	8.21	4.04			
		4.18			
Pro[9]		4.46	1.97	2.03	3.65[a]
			2.31		
Ser[10]	8.46	4.42	3.87		
			3.92		
Asp[11]	8.37	4.68	2.85[a]		
Met[12]	8.12	4.36	1.91	2.37	
			1.94		
Tyr[13]	8.05	4.61	2.92		
			3.09		
Val[14]	7.90	4.02	2.00	0.85	
				0.88	
His[15]	8.49	4.67	3.14		
			3.28		

Arg[1]-NH-C(δ): 7.23 ppm; Arg[1]-NH-C(ε): ~6.7 ppm (broad).
Ile[3]-CH_3-C(β): 0.90 ppm; Ile[4]-CH_3-C(β): 0.90 ppm.
Met[12]-H-C(ε): 2.05 ppm.
Tyr[13]-H-C(2′,6′): 7.11 ppm; Tyr[13]-H-C(3′,5′): 6.80 ppm.
His[15]-H-C(2′): 7.31 ppm; His[15]-H-C(4′): 8.62 ppm; His[15]-NH_{ring}: 7.20 ppm; His[15]-CO-NH_2: 7.55 ppm

[a] Close AB system

[b] Shift values are interchangeable

present to a little extent in a conformation different from the random coil arrangement. From this we conclude that peptide fragments useful for the achievement of the goal defined in the introduction have to contain more amino acid residues, although defined spatial arrangements are known from oligopeptides of comparable size [21]. Investigations on the synthesis and NMR spectroscopic analysis of larger peptides resembling the wild type as well as modified cleavage regions of the human rhinovirus are in progress.

Table 2. ^{13}C chemical shifts of **1** in H_2O:D_2O = 4 : 1 (3 m*M*) at 300 K relative to external *TMS*

	α	β	γ	δ	CO
Arg[1]	55.74	31.21	27.45	44.78	172.26
Pro[2]	64.67	33.76[a]	29.04	52.34	177.81
Ile[3]	62.79	40.35	29.04	14.15[b]	177.71
Ile[4]	62.22	40.35	28.85	14.36[b]	177.87
Thr[5]	63.08[c]	71.39[d]	23.03[e]		176.06
Thr[6]	63.12[c]	71.40[d]	23.09[e]		175.56
Ala[7]	53.96	21.14			179.15
Gly[8]	46.09				173.56
Pro[9]	65.03	33.78[a]	28.85	51.44	179.05
Ser[10]	60.21	65.18			176.23
Asp[11]	54.83	40.05[f]			176.85
Met[12]	57.53	34.27	33.38		177.41
Tyr[13]	59.16	39.99[f]			177.21
Val[14]	63.94	34.40	22.15		177.26
			22.53		
His[15]	56.47	30.57			178.21

Arg[1]-C(ε): 161.07 ppm.
Ile[3]-CH_3-C(β): 19.07[g] ppm; Ile[4]-CH_3-C(β): 19.10[g] ppm.
Asp[11]-COOH: 179.15 ppm.
Met[12]-C(ε): 18.37 ppm.
Tyr[13]-C(1′): 132.38 ppm; Tyr[13]-C(2′,6′): 134.81 ppm; Tyr[13]-C(3′,5′): 119.79 ppm; Tyr[13]-C(4′): 158.79 ppm.
His[15]-C(1′): 132.78 ppm; His[15]-C(2′): 121.64 ppm; His[15]-C(4′): 137.83 ppm
[a–g] Shift values are interchangeable

Experimental

The synthesis of the peptides was carried out using the solid phase peptide synthesis method [22]. The crude peptides were purified by reversed phase HPLC using aqueous trifluoroacetic acid (0.1%) and acetonitrile as the mobile phase. Identity and homogeneity were assessed by HPLC analysis, FAB mass spectrometry, and amino acid analysis.

NMR measurements were performed in degassed neutral aqueous solutions (H_2O:D_2O = 4 : 1) at 300 K on a Bruker AM 400 WB NMR spectrometer operating at 9.4 T and equipped with an inverse probe for the proton-detected heteronuclear experiments. Sample concentrations were 3 m*M* (**1**) and 12 m*M* (**2**), respectively. The water resonance was saturated by an appropriate RF field. For this purpose and for performing the DQF-COSY experiment with O1/O2 coherence, the software supplied by the manufacturer had to be modified slightly in some cases. All spectra with the exception of the long-range C,H-COSY experiment were recorded in the phase-sensitive mode using the TPPI method [23]. Typical measurement times were 14 hours for the DQF-COSY and C,H-COSY experiments and 64 hours for all other experiments, but a C,H-COSY spectrum of **2** containing virtually all necessary information could be achieved in about 2 hours. Data were processed on a satellite station (Bruker Aspect X 32) using the UXNMR software [24]. Signal to noise improvement was achieved by submitting the processed data to the AURELIA algorithm [25]. No symmetrization procedure was applied to COSY and NOESY spectra.

Table 3. ^{1}H chemical shifts of **2** in H_2O:D_2O = 4 : 1 (12 m*M*) at 300 K relative to external *TMS*

	NH	α	β	γ	δ
Ile[1]		3.87	1.90	1.12	0.81
				1.41	
Val[2]	8.48	4.19	1.99	0.88	
				0.92	
Thr[3]	8.34	4.28	~4.1	1.12	
Arg[4]	8.28	4.28	1.64	1.60	3.14
			1.78		
Pro[5]		4.37	1.94	1.94	3.55
			2.22		3.74
Ile[6]	8.22	4.07	1.77	1.12	0.84
				1.43	
Ile[7]	8.20	4.22	1.80	1.12	0.77
				1.38	
Thr[8]	8.24	4.33	~4.1	1.03[a]	
Thr[9]	7.98	4.24	~4.1	1.05[a]	
Tyr[10]	8.16	4.60	2.86		
			3.06		
Gly[11]	8.12	3.99			
		4.05			
Pro[12]		4.37	1.94	1.94	3.55
			2.26		3.74
Ser[13]	8.38	4.38	3.80		
			3.85		
Asp[14]	8.32	4.64	2.67		
			2.85		
Met[15]	8.17	4.38	1.99	2.45	
			2.07	2.55	

Ile[1]-CH_3-C(β): 0.89 ppm; Ile[6]-CH_3-C(β): 0.81 ppm; Ile[7]-CH_3-C(β): 0.81 ppm.
Arg[4]-NH-C(δ): 7.13 ppm; Arg[4]-NH-C(ε): ~6.6 ppm (broad).
Tyr[10]-H-C(2′,6′): 7.07 ppm; Tyr[10]-H-C(3′,5′): 6.75 ppm.
Met[15]-H-C(ε): 2.03 ppm; Met[15]-CO-NH_2: 7.45 ppm.
[a] Shift values are interchangeable

J-modulated 1 D ^{13}C experiment (SEFT, [26]): sweep width, 25 kHz; size, 64 k data points; relaxation delay, 3 s; pulse width (90°), 5.1 μs; filter function, exponential weighting; line broadening factor, 2 Hz.

Double-quantum filtered H,H-COSY [23], modified for solvent presaturation using O1/O2 coherence: sweep width, 3.5 kHz; size, 2 k data points in ω_2, 512 experiments in ω_1 (32 scans); relaxation delay, 1.8 s; pulse width (90°), 12.2 μs; zero filling, 2 k × 2 k data points (real); filter function, sine bell squared shifted by π/3 rad in both dimensions.

NOESY with solvent presaturation using O1/O2 coherence [27]: sweep width, 3.5 kHz; size, 2 k data points in ω_2, 512 experiments in ω_1 (64 scans); relaxation delay, 1.3 s; pulse width (90°), 12.0 μs; mixing time, various values between 100 and 800 ms; zero filling, 2 k × 2 k data points (real); filter function, sine bell squared shifted by π/3 rad in both dimensions.

Table 4. ^{13}C chemical shifts of **2** in H_2O:D_2O = 4 : 1 (12 m*M*) at 300 K relative to external *TMS*

	α	β	γ	δ	CO
Ile[1]	62.11	40.96	28.55	14.47	173.85
Val[2]	64.16	34.46	22.38		177.57
			22.71		
Thr[3]	63.35	71.53	23.35		175.67
Arg[4]	55.56	32.08	28.37	45.12	175.59
Pro[5]	64.70[a]	33.81	28.90[b]	52.37	178.22
Ile[6]	62.89	40.39[c]	28.55	14.90	177.91
Ile[7]	62.41	40.45[c]	28.55	14.26	177.91
Thr[8]	63.41	71.53	23.11[d]		175.99
Thr[9]	63.26	71.53	23.14[d]		175.51
Tyr[10]	59.36	40.82			177.50
Gly[11]	46.34				173.48
Pro[12]	65.19[a]	33.81	29.05[b]	51.53	179.17
Ser[13]	60.29	65.42			176.21
Asp[14]	55.25	40.82			177.07
Met[15]	57.07	34.53	33.81		180.66

Ile[1]-CH_3-C(β): 18.46 ppm; Ile[6]-CH_3-C(β): 19.18[e] ppm; Ile[7]-CH_3-C(β): 19.20[e] ppm.
Arg[4]-C(ε): 161.34 ppm.
Tyr[10]-C(1′): 132.55 ppm; Tyr[10]-C(2′,6′): 134.94 ppm; Tyr[10]-C(3′,5′): 119.91 ppm; Tyr[10]-C(4′): 158.92 ppm.
Asp[14]-COOH: 179.70 ppm.
Met[15]-C(ε): 18.53 ppm.
[a–e] Shift values are interchangeable

Reverse C,H-COSY with BIRD sequence and GARP1 decoupling [28], modified for solvent presaturation during both relaxation and BIRD delay: sweep width, 18 kHz in ω_1, 3 kHz in ω_2; size, 2 k data points in ω_2, 256 experiments in ω_1 (128 scans); relaxation delay, 1 s; BIRD delay, 0.3 s; pulse width (90°), 10.9 μs (^1H), 8.6 μs (^{13}C hard), 55 μs (^{13}C soft); zero filling, 2 k × 1 k data points (real); filter function, sine bell squared shifted by π/2 rad in both dimensions.

Long-range reverse C,H-COSY with *J*-filter [29], modified for solvent presaturation: sweep width, 22 kHz in ω_2, 3.5 kHz in ω_1; size, 2 k data points in ω_2, 512 experiments in ω_1 (240 scans); relaxation delay, 1 s; pulse width (90°), 10.9 μs (^1H), 8.6 μs (^{13}C); *J*-filter delay, 3.57 ms (optimized for suppression of one-bond C,H couplings); delay for evolution of long range couplings, 50 ms (optimized for J = 10 Hz); zero filling, 2 k × 2 k data points (real); filter function, sine bell squared shifted by π/2 rad in both dimensions; magnitude representation.

Relayed reverse C,H-COSY with BIRD sequence [30], modified for solvent presaturation during both relaxation and BIRD delay: sweep width, 18 kHz in ω_2, 3.5 kHz in ω_1; size, 2 k data points in ω_2, 512 experiments in ω_1 (272 scans); relaxation delay, 1 s; BIRD delay, 0.3 s; pulse width (90°), 10.9 μs (^1H), 8.6 μs (^{13}C); zero filling, 2 k × 2 k data points (real); filter function, sine bell squared shifted by π/2 rad in both dimensions.

Acknowledgements

This work was supported by the Fonds zur Förderung der wissenschaftlichen Forschung in Österreich (Project No. P 6537 C). H. K. and M. K. are grateful to Mag. H.-P. Kählig for assistance with the Aspect X 32 computer and for stimulating discussions.

References

[1] Wimmer E. (1989) Proteolytic Processing in Viral Replication. In: Curr. Commun. Mol. Biol.. Cold Spring Harbor Laboratory Press, p. 1
[2] Nicklin M. J. H., Toyoda H., Murray M. G., Wimmer E. (1986) Biotechnol **4**: 33
[3] Hellen C. U. T., Kräusslich H.-G., Wimmer E. (1989) Biochemistry **28**: 9881
[4] Palmenberg A. C. (1990) Annu. Rev. Microbiol. **44**: 603
[5] Rueckert R. R. (1990). In: Fields B. N. (ed.) Virology, 2nd ed., Vols. 1 and 2. Raven press, New York, p. 507
[6] Hanecak R., Semler B., Anderson C., Wimmer E. (1982) Proc. Natl. Acad. Sci. USA **79**: 3973
[7] Sommergruber W., Zorn M., Blaas D., Fessl F., Volkmann P., Maurer-Fogy I., Pallai P., Merluzzi V., Matteo M., Skern T., Küchler E. (1989) Virology **169**: 68
[8] Toyoda H., Nicklin M. J. H., Murray M. G., Anderson C. W., Dunn J. J., Studier F. W., Wimmer E. (1986) Cell **45**: 761
[9] Ypma-Wong M. F., Dewalt P. G., Johnson V. H., Lamb J. G., Semler B. (1988) Virology **166**: 265
[10] Gorbalenya A. E., Blinov V. M., Donchenko A. M. (1986) FEBS Lett. **194**: 253
[11] Bazan J. F., Fletterick R. J. (1988) Proc. Natl. Acad. Sci. USA **85**: 7872
[12] Bazan J. F., Fletterick R. J. (1989) FEBS Lett. **249**: 5
[13] Skern T., Sommergruber W., Auer H., Volkmann P., Zorn M., Liebig H.-D., Fessl F., Blaas D., Küchler E. (1991) Virology **181**: 46
[14] Johnston M. I., Allaudeen H. S., Sarver N. (1989) Trends Pharmacol. Sci. **10**: 305
[15] Ovchinnikov Yu. A., Ivanov V. T. (1975) Tetrahedron Lett. **31**: 2177
[16] Zieger G., Andreae F., Sterk H. (1991) Magn. Reson. Chem. **29**: 580 and refs. cited therein
[17] Wüthrich K. (1986). In: NMR of Proteins and Nucleic Acids. Wiley, New York
[18] Kessler H., Loosli H.-R. Oschkinat H. (1985) Helv. Chim. Acta **68**: 661
[19] Kessler H., Gehrke M., Griesinger C. (1988) Angew. Chem. **100**: 507
[20] Hofmann M., Gehrke M., Bermel W., Kessler H. (1989) Magn. Reson. Chem. **27**: 877
[21] Wemmer D., Kallenbach N. R. (1983) Biochemistry **1983**: 1901
[22] Merrifield R. B. (1963) J. Am. Chem. Soc. **85**: 2149
[23] Marion D., Wüthrich K. (1983) Biochem. Biophys. Res. Commun. **113**: 967; Rance M., Sørensen O. W., Bodenhausen G., Wagner G., Ernst R. R., Wüthrich K. (1983) ibid. **117**: 479
[24] Fa. Bruker Analytische Meßtechnik GmbH, Karlsruhe, FRG; software release 10/90
[25] Neidig K. P., Kalbitzer H. R. (1990) J. Magn. Reson. **88**: 155
[26] Brown D. W., Nakashima T. T, Rabenstein D. L. (1981) J. Magn. Reson. **45**: 302
[27] Bodenhausen G., Kogler H., Ernst R. R. (1984) J. Magn. Reson. **58**: 370
[28] Bax A., Subramanian S. (1986) J. Magn. Reson. **67**: 565
[29] Bax A., Summers M. F. (1986) J. Am. Chem. Soc. **108**: 2093
[30] Lerner L., Bax A. (1986) J. Magn. Reson. **69**: 375

Received October 15, 1991. Accepted November 5, 1991